due to their water equivalency (i.e. they cannot be differentiated from tissue), but accurate localization is necessary for comparison of measured dose to dose calculated on CT images.
Materials and Methods: We constructed two mock PSDs with CT-radio-opaque metal wire used in place of scintillating fibers. Each mock detector was constructed to the specifications of *in-vivo* PSDs being used at our institution and consisted of a 7 mm graphite spacer, 2 mm of radio-opaque wire coupled to a clear plastic optical fiber contained in black polyethylene jacketing. 2 mm spherical ceramic fiducials were attached at the end of the detector and to either side of the detector 1 cm distal to the wire as surrogates for calculating the location of the 'sensitive volume'. The detectors were attached to an endorectal balloon which was subsequently inserted into an anthropomorphic prostate phantom and inflated. A CT scan (2.5 mm slice thickness, the same used when imaging *in-vivo* detectors in patients) of the phantom was then acquired, and the resulting images imported into the Pinnacle treatment planning system. A script then determined the location of the active volume by calculating a line between the center of the proximal fiducial and a point halfway between the two distal fiducials (i.e. the center of the optical fiber) and contouring 1 mm diameter circles around the line on slices containing the portion of the line between 8 mm and 10 mm. The locations of the resulting contours were compared to the location of the metal wire. This process was repeated ten times – removing and deflating the balloon, detaching the detectors, and then re-setting up the experiment completely each time.
Results: The average deviation in the axial plane between the center of the contours and the center of the metal wire was 0.1 mm in the anterior direction (Figure 1). The root-mean-square deviation was 0.4 mm. All contours were within 0.8 mm of the actual location. 13 out of 20 measurements were localized to the correct axial slice, and the other 7 were one slice off. Axial discrepancies were considered more important than SI discrepancies because the dose gradient of patient treatment plans lies primarily along the AP direction. The direction and magnitude of the deviation from actual location for all 20 measurements are shown in Figure 1.

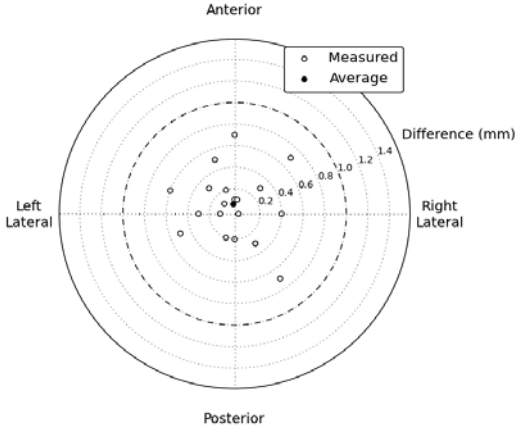

Conclusions: The methodology for contouring the sensitive volume of a scintillation detector was found to consistently produce contours in good agreement with the position of the detector's sensitive volume. This method can be used to effectively localize the actual PSDs within an accuracy of less than 0.8 mm.

PO-0769
Flattening filter free beam dosimetry with organic scintillators, ionization chambers and diamonds
A.R. Beierholm[1], C.F. Behrens[2], C.E. Andersen[1]
[1]*Center for Nuclear Technologies, Technical University of Denmark, Roskilde, Denmark*
[2]*Department of Oncology R, Copenhagen University Hospital Herlev, Copenhagen, Denmark*

Purpose/Objective: Medical linear accelerators (linacs) capable of delivering flattening filter free (FFF) beams present a promising option for radiotherapy clinics due to potentially reduced treatment times and lower doses out of field. However, successful treatment outcome depends on the accuracy of the commissioning data loaded into treatment planning systems - especially for treatments involving small or composite fields. A comparison of beam data between dosimetry methods is therefore required to assess the uncertainties on dose estimates. Differences in response of different dosimetry methods, primarily due to energy dependence, have been discussed in the literature for conventional flattened (FF) beams. However, it is not obvious that the same differences apply in FFF beams. To assess this, we present measurements of central dosimetric parameters, obtained using three different dosimetry methods in FFF beams.
Materials and Methods: Measurements were performed in water for a Varian TrueBeam not yet commissioned for FFF beams. The measurements concerned i) output factors, ii) TPR20:10 ratios, and iii) dose per pulse. Output factors and TPR20:10 measurements were acquired for 6 MV and 10 MV beams operated in FFF mode, using i) a fibre-coupled organic scintillator, ii) a PTW 60003 diamond detector and iii) an IBA CC13 ionization chamber. To accurately determine the increase in instantaneous dose rate when removing the flattening filter, the dose per pulse was measured using the fibre-coupled organic scintillator for FFF as well as FF beams.
Results: The table shows measured output factors (mean ± 1 SD) obtained at 90 cm source to surface distance and 10 cm depth. Differences between detectors were significant for large fields, amounting to 3.2 % at the largest. Conversely, differences of up to 2.8 % between the scintillator and diamond were seen for small fields. Measurements of TPR20:10 ratios were more consistent, agreeing to within 0.8 % for the three dosimetry methods. The measured dose per pulse was 2.7 times higher for 6 MV FFF than for 6 MV FF, and 4.6 times higher for 10 MV FFF than for 10 MV FF, comparing well with literature values of FFF beam output (Int J Radiat Oncol Biol Phys 80, 1228-1237, 2011).
Conclusions: The presented measurements show that detector-inherent differences in output factor measurements are also encountered in FFF beams. The over-response of diamonds has been discussed in the literature for FF beams (Phys Med Biol 57, 4461-4476, 2012); similarly, differences between ionization chambers and scintillators have been reported for 6 MV large fields (Med Phys 38, 2140-2150, 2011). We conclude that these findings also apply in FFF beams. However, the needed correction factors for ionization chambers and diamonds are larger for FFF beams due to the higher dose per pulse. To further assess dosimetric uncertainties, a logical next step would be to compare beam data for linacs situated at different clinics, obtained using the same set of equipment.

Beam	Field size	Dosimeter		
	[cm x cm]	Scintillator	Diamond	CC13
6 MV FFF	1 x 1	0.699 ± 0.003	0.708 ± 0.001	-
	2 x 2	0.813 ± 0.003	0.800 ± 0.002	0.798 ± 0.001
	3 x 3	0.854 ± 0.003	0.839 ± 0.002	0.845 ± 0.001
	5 x 5	0.913 ± 0.002	0.899 ± 0.002	0.905 ± 0.001
	10 x 10	1.000 ± 0.002	1.000 ± 0.001	1.000 ± 0.001
	20 x 20	1.077 ± 0.004	1.095 ± 0.003	1.088 ± 0.001
	30 x 30	1.110 ± 0.005	1.143 ± 0.003	1.126 ± 0.001
	40 x 40	1.125 ± 0.003	1.162 ± 0.002	1.142 ± 0.001
10 MV FFF	1 x 1	0.670 ± 0.008	0.689 ± 0.002	-
	2 x 2	0.834 ± 0.002	0.830 ± 0.002	0.811 ± 0.001
	3 x 3	0.888 ± 0.003	0.884 ± 0.002	0.880 ± 0.001
	5 x 5	0.938 ± 0.002	0.930 ± 0.002	0.938 ± 0.001
	10 x 10	1.000 ± 0.002	1.000 ± 0.002	1.000 ± 0.001
	20 x 20	1.049 ± 0.003	1.051 ± 0.003	1.050 ± 0.001
	30 x 30	1.072 ± 0.003	1.075 ± 0.003	1.069 ± 0.001
	40 x 40	1.078 ± 0.003	1.087 ± 0.003	1.078 ± 0.001

PO-0770
A uniformity correction protocol for Radiochromic film dosimetry in TomoTherapy QA.
M. Maddalo[1], R. Avitabile[2], M. Buglione di Monale[3], S. Tonoli[3], G. Gandinelli[3], L. Spiazzi[2]
[1]*Milan University, Medicine, Milano, Italy*
[2]*Spedali Civili, Medical Physics, Brescia, Italy*
[3]*Brescia University, Radiation Oncology, Brescia, Italy*

Purpose/Objective: EBT2 and EBT3 radiochromic films are characterized by a high spatial resolution that can't be matched by two-dimensional ion chamber or diode arrays. Thanks to this property they seem to be ideal dosimeters for the verification of TomoTherapy stereotactic body radiation therapy (SBRT) plans. Their response is degraded by two different sources: acquisition process related distortion; inherent dose sensitivity variations. Moreover this non-uniformities convolve with the regular dose fluctuation pattern inherent to helical dose delivery. In this study a protocol that allows to reduce the spatial non-uniformity to a clinically acceptable level was investigated.
Materials and Methods: Dose sensitivity variations was quantified for different film batches by delivering a uniform dose distribution with a standard linear accelerator. The frequency range that characterized noise bands was identified with a band-pass filter. 10 TomoTherapy SBRT plans were delivered on EBT2-3 films. Films were digitized with an Epson scanner and the resulting images were converted in net

optical density (OD). The optical density distributions were then corrected for the acquisition-related distortion by means of an algorithm available in literature. The dose fluctuation pattern inherent to helical TomoTherapy was then extracted by applying another band-pass filter. Finally, after the application of an OD-dose calibration, the dose distributions were filtered in order to reduce low and high frequency noise. For the selection of the most suitable filter various possibilities were tested, including the complete removal of the predetermined frequency range which characterizes the batch. The quality of the uniformity correction protocol was evaluated by comparing passing rates obtained with films and those achieved with PTW OCTAVIUS system.
Results: The level of dose sensitivity variations depends on the specific batch [2-4] %. The frequency range seems to be similar for intra-batch films, while different for inter-batch films. The pure elimination of the band frequency range is not applicable. This is because the frequencies that characterized the dose sensitivity variations and those that characterized the dosimetric information are comparable. The best low and high frequency noise reduction is obtained by applying the wavelet filtering method and separately adding the dose fluctuation pattern inherent to helical TomoTherapy to the SBRT dose distribution. Using a gamma function 3mm-3%, agreement between planned and measured dose distributions was found to be always better then 90% only if the correction protocol was applied.

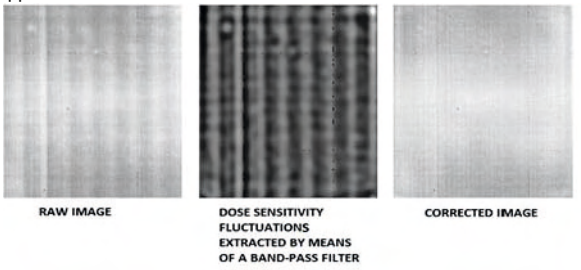

Conclusions: Radio chromicfilms response, if corrected by our protocol, can be used for the verification of TomoTherapy SBRT plans where high spatial resolution is needed.

POSTER: PHYSICS TRACK: DOSE MEASUREMENTS

PO-0771
A reliable algorithm for calculating 3D patient dose based on measured point doses in a QA phantom
A. Gustafsson[1], P. Münger[2], T. Matzen[2], G. Nilsson[2]
[1]*Cureos AB, Uppsala, Sweden*
[2]*ScandiDos AB, Uppsala, Sweden*

Purpose/Objective: QA phantoms for dose verification of complex radiation treatments such as IMRT and VMAT are currently in widespread use. By monitoring beam or control point dose in a large number of small detectors distributed within the QA phantom and comparing measured dose with TPS calculated dose *in the QA phantom*, accurate confirmation of spatial deviations between planned and delivered dose can be obtained.The clinical interpretation of deviations is however limited by the fact that doses are being compared in the QA phantom. To facilitate evaluation of the clinical impact of observed dose deviations, the TPS calculated dose *in the patient* should ideally be compared with the patient dose distribution *corresponding to* the measured doses in the QA phantom.
Materials and Methods: This work describes the development and validation of a novel technique for accurate and reliable 3D photon dose calculation in a patient volume based on detector dose measurements in a QA phantom of arbitrary material. The technique consists of two steps:
1. For the given beam quality and accounting for the phantom composition, estimate the 2D energy fluence distribution that best represents the measured detector doses in the QA phantom.
2. Apply the obtained energy fluence and the given beam quality in a 3D dose calculation for the patient volume.
The estiated energy fluence distribution represents the radiant energy resulting from modulation and collimation in the treatment head,independent of dose calculation geometry. Presence or absence of flattening filter is automatically accounted for.
The energy fluence estimation is formulated as a linear optimization problem, where the objective is to minimize the integral fluence given that the calculated phantom dose in every accountable detector position is greater than or equal to the measured dose. This formulation is guaranteed to have a feasible solution and the calculated-to-measured dose deviation is implicitly minimized through the integral fluence objective.
Results: The technique has been applied to both MLC collimated IMRT fields with non-uniform energy fluence and VMAT fields where patient dose is calculated for the individual control points and subsequently added to yield a total 3D dose. The technique is consistently able to reproduce reference absolute dose results within 3% and 3 or 6 mm, depending on the local spatial resolution of the detector grid.
Conclusions: A technique for calculating 3D photon dose in the patient volume based on measured detector doses in a QA phantom has been implemented. The technique is applicable to complex treatments such as IMRT and VMAT and has been shown to accurately and reliably obtain 3D patient dose distributions that can be immediately compared with 3D dose distributions planned and calculated with a regular treatment planning system.

PO-0772
Applicability of AAPM TG 119 on a 3D dosimetric phantom
A.F. Monti[1], L. Trombetta[1], M.G. Brambilla[1], C. Carbonini[1], M.B. Ferrari[1], C. Cadioli[1], H.S. Mainardi[1], A. Torresin[1]
[1]*Azienda Ospedaliera Ospedale Niguarda Ca'Granda, Medical Physics, Milan, Italy*

Purpose/Objective: Treatment planning system (TPS) capabilities should beverified in a real 3D situation with rigorous procedures, both for static and rotational modulated fields.
The American Association of Physicists in Medicine TaskGroup 119 (TG119) proposed a water equivalent square slab phantom (30x30x15 cm^3) with four IMRT tests: mock prostate (MP), head-and-neck (HN), C-shaped target (CS), and Multi Target (MT). Each test was developed to assess the overall accuracy of planning and delivery of IMRT treatments. The test suite with DICOM-RT images and structures can be downloaded from the AAPM web-site. TG119 defines also beams arrangement, IMRT goals, and methods for analyzing the dosimetric results on their phantom. The AAPM phantom is cheap and easily reproducible in every department, but it allows only single point or single planar measurements. In order to apply the TG119 report in a more sophisticated situation we used a 3D dosimetric phantom and all tests were re-optimized to satisfy all defined goals.
Materials and Methods: TG119 was pre-emptively used 'as is' in order to test the capability of our clinical arrangement. After this, TG119 structures were superimposed on the CT images of a cylindrical PMMA phantom surrounding two orthogonal matrix with 1069 total diodes (Delta4 - 3D dosephantom; Scandidos, SWE). TG119 tests were thus calculated and optimized using a Monte Carlo TPS (Monaco3.20; Elekta, SWE) for 6 and 10 MV photon beams, with IMRT and VMAT techniques, following the plan proposed goals. Delta4 phantom was used in order to carryout comparison between measured and planned 3D absolute dose distributions. A 3%, 3mm with a 10% threshold (defined by the isodose line representing 10% of maximum dose) gamma test was performed for plans analysis.
Results: Goals proposed in TG119 were satisfied for each planand technique. For all IMRT plans gamma values were lower than 1 for more than 98.3% of compared point, except for the CS plan delivered with 6 MV (Fig.1), where gamma analysis was satisfied for 90.5% of total points. The mean percentage of passing points for all energies was 98.4 ± 3.3%. Preliminary results were obtained for VMAT cases, with a mean percentage of 88.5 ± 8.4%. VMAT is at present under refinement and better results are expected after the optimisation of the Monte Carlo model.